

Geophysical Research Letters[®]

RESEARCH LETTER

10.1029/2022GL098600

Special Section:

Results from Juno's Flyby of Ganymede

Key Points:

- Hubble Space Telescope observations of Ganymede's orbitally trailing hemisphere on 7 June 2021 in support of Juno flyby
- Brightness ratio of northern and southern auroral ovals oscillates such that the oval facing the Jovian plasma sheet is brighter
- Oscillation suggests the aurora is driven by magnetic stresses coupling the moon's magnetic field to the surrounding Jovian plasma sheet

Supporting Information:

Supporting Information may be found in the online version of this article.

Correspondence to:

J. Saur,
saur@geo.uni-koeln.de

Citation:

Saur, J., Duling, S., Wennmacher, A., Willmes, C., Roth, L., Strobel, D. F., et al. (2022). Alternating north-south brightness ratio of Ganymede's auroral ovals: Hubble Space Telescope observations around the Juno PJ34 flyby. *Geophysical Research Letters*, 49, e2022GL098600. <https://doi.org/10.1029/2022GL098600>

Received 30 MAR 2022

Accepted 11 AUG 2022







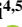


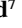







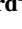
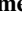
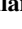
Author Contributions:

Data curation: Joachim Saur, Alexandre Wennmacher, Clarissa Willmes, Lorenz Roth, Darrell F. Strobel, Fran Bagenal, Scott J. Bolton, Bertrand Bonfond, George Clark, Randy Gladstone, Denis C. Grodent, Candice J. Hansen, Glenn S. Orton, Kurt D. Retherford, Abigail M. Rymer

© 2022. The Authors.

This is an open access article under the terms of the [Creative Commons Attribution-NonCommercial License](https://creativecommons.org/licenses/by-nc/4.0/), which permits use, distribution and reproduction in any medium, provided the original work is properly cited and is not used for commercial purposes.

Alternating North-South Brightness Ratio of Ganymede's Auroral Ovals: Hubble Space Telescope Observations Around the Juno PJ34 Flyby

Joachim Saur¹ , Stefan Duling¹ , Alexandre Wennmacher¹ , Clarissa Willmes¹ , Lorenz Roth² , Darrell F. Strobel³ , Frédéric Allegrini^{4,5} , Fran Bagenal⁶ , Scott J. Bolton⁴ , Bertrand Bonfond⁷ , George Clark⁸ , Randy Gladstone^{4,5} , Thomas K. Greathouse⁴ , Denis C. Grodent⁷ , Candice J. Hansen⁹ , William S. Kurth¹⁰ , Glenn S. Orton¹¹ , Kurt D. Retherford^{4,5} , Abigail M. Rymer⁸ , and Ali H. Sulaiman¹⁰ 

¹Institute of Geophysics and Meteorology, University of Cologne, Cologne, Germany, ²School of Electrical Engineering, KTH, Royal Institute of Technology, Stockholm, Sweden, ³Johns Hopkins University, Baltimore, MD, USA, ⁴Southwest Research Institute, San Antonio, TX, USA, ⁵Department of Physics and Astronomy, University of Texas at San Antonio, San Antonio, TX, USA, ⁶University of Colorado, Boulder, CO, USA, ⁷Université de Liège, LPAP - STAR Institute, Liège, Belgium, ⁸Applied Physics Laboratory Johns Hopkins University, Laurel, MD, USA, ⁹Planetary Science Institute, Tucson, AZ, USA, ¹⁰Department of Physics and Astronomy, University of Iowa, Iowa City, IA, USA, ¹¹Jet Propulsion Laboratory, California Institute of Technology, Pasadena, CA, USA

Abstract We report results of Hubble Space Telescope observations from Ganymede's orbitally trailing side which were taken around the flyby of the Juno spacecraft on 7 June 2021. We find that Ganymede's northern and southern auroral ovals alternate in brightness such that the oval facing Jupiter's magnetospheric plasma sheet is brighter than the other one. This suggests that the generator that powers Ganymede's aurora is the momentum of the Jovian plasma sheet north and south of Ganymede's magnetosphere. Magnetic coupling of Ganymede to the plasma sheet above and below the moon causes asymmetric magnetic stresses and electromagnetic energy fluxes ultimately powering the auroral acceleration process. No clear statistically significant timevariability of the auroral emission on short time scales of 100s could be resolved. We show that electron energy fluxes of several tens of mW m⁻² are required for its OI 1,356 Å emission making Ganymede a very poor auroral emitter.

Plain Language Summary Jupiter's moon Ganymede is the largest moon in the solar system and the only known moon with an intrinsic magnetic field and two auroral ovals around its north and south poles. Earth also possesses two auroral ovals, which are bands of emission around its poles. This emission is also referred to as northern and southern lights. We use the Hubble Space Telescope to observe Ganymede's aurora around the time when NASA's Juno spacecraft had a close flyby at Ganymede. We find that the brightness of the northern and southern ovals alternate in intensity with a period of 10 hr. Additionally, we derive that an energy flux of several tens of milli-Watt per square meter is necessary to power the auroral emission. This energy flux comes from energetic electrons accelerated in the vicinity of Ganymede.

1. Introduction

With its intrinsic magnetic field and two auroral ovals, Jupiter's moon Ganymede resembles other planets with intrinsic magnetic fields and auroral emission (Hall et al., 1998; Kivelson et al., 1996, 1998; Feldman et al., 2000). The key difference compared to magnetized planets is that Ganymede's mini-magnetosphere is located within Jupiter's gigantic magnetosphere and does not possess a bow shock. However, many processes of Ganymede's unique magnetosphere such as the mechanisms that power its aurora are still poorly understood. The return of the Juno spacecraft to Ganymede on 7 June 2021, 20 years after the Galileo mission thus provides a great opportunity to further our understanding of the moon. Juno passed Ganymede on its 34th perijove orbit (PJ34) primarily across its orbitally leading side, that is, the downstream side of its magnetosphere. In support of the Juno flyby, Hubble Space Telescope (HST) observations with the Space Telescope Imaging Spectrograph (STIS) camera were obtained. HST observed Ganymede on three HST orbits before and three orbits after Juno's closest approach to monitor the evolution of the aurora. Simultaneous observations were not possible due to scheduling constraints of HST as detailed in Section 2.

Investigation: Joachim Saur, Stefan Duling, Lorenz Roth, Darrell F. Strobel, Frédéric Allegrini, Bertrand Bonfond, Denis C. Grodent

Writing – review & editing: Joachim Saur, Stefan Duling, Alexandre Wennmacher, Lorenz Roth, Darrell F. Strobel, Frédéric Allegrini, Bertrand Bonfond, George Clark, Randy Gladstone, Thomas K. Greathouse, Denis C. Grodent, William S. Kurth, Glenn S. Orton, Kurt D. Retherford, Ali H. Sulaiman

Ganymede's auroral emission was detected with HST/GHRS (Hall et al., 1998) and provided the first evidence that Ganymede possesses a thin molecular oxygen atmosphere. A recent analysis of multiple sets of HST data showed that Ganymede additionally harbors a sublimation-driven localized water atmosphere (Roth et al., 2021). Spatially resolved observations with HST/STIS have demonstrated that Ganymede's emission primarily stems from two auroral structures around its north and south poles (Feldman et al., 2000; McGrath et al., 2013). The overall brightness and the location of the aurora changes periodically with Ganymede's position in Jupiter's magnetosphere (Musacchio et al., 2017; Saur et al., 2015). The total brightness is maximum when Ganymede is in the center of Jupiter's magnetospheric plasma sheet. Based on McGrath et al. (2013), and Greathouse et al. (2022), the auroral ovals match to regions near the open-closed field line region of Ganymede's mini-magnetosphere and delineate locations where the transition from closed to open field lines of Ganymede's mini-magnetosphere occurs. Along these field line regions a yet unidentified mechanism accelerates particles that precipitate into Ganymede's tenuous atmosphere and excite the observed emission. Various possible mechanisms are discussed in the literature (e.g., Eviatar et al., 2001). For example, acceleration might be due to reconnection, that is, merging of Jupiter's and Ganymede's magnetic field lines at the open-closed field line boundary. This process converts magnetic field energy into kinetic energy of the particles. Alternatively, field-aligned electric currents connecting into Ganymede's ionosphere might be related to particle acceleration. Another possibility would be that electro-magnetic waves accelerate particles which appears to be the dominant acceleration mechanism for Jupiter's main aurora (Mauk et al., 2017; Saur et al., 2018). A basic understanding of the aurora is of fundamental interest, but it is also important because the dynamics of its auroral ovals have been used to deduce a subsurface ocean within Ganymede (Saur et al., 2015). A better understanding of Ganymede's auroral emission will also provide important information for the science planning of ESA's JUICE mission, which will orbit Ganymede starting 2032 (e.g., Grasset et al., 2013).

2. Data and Data Processing

The HST observations were acquired in support of the Juno flyby and monitored Ganymede's orbitally trailing side on 7 June 2021. The observations were carried out with HST/STIS with grating G140 L and aperture 52X2. Details of the exposures are given in Table S1 in Supporting Information S1. STIS provides spectral images of Ganymede's emission at several different wavelengths. In this work we analyze Ganymede's auroral OI emission at 1,356 Å because Ganymede's auroral emission at this wavelength is about a factor of two brighter than the other oxygen FUV OI emission at 1,304 Å (Feldman et al., 2000). At OI 1,304 Å in addition to auroral emission there is solar-resonance scattering and surface-reflected emission as well. OI 1,356 Å is a semi-forbidden multiplet and hence an optically thin emission, almost entirely auroral, leading to a superior signal-to-noise ratio (SNR) from OI 1,356 Å in comparison to OI 1,304 Å. The HST data were processed identically to previous analyses of Ganymede's observations obtained with STIS (e.g., Musacchio et al., 2017; Saur et al., 2015). The main steps are: Determination of the location of Ganymede within each spectral image, removal of the solar reflected light from the surface and rotation of the resultant spectral image such that Jupiter north is up. The observations consist of two visits with three HST orbits each (see Table S1 in Supporting Information S1). In Figure 1, we display the scheduling of the HST observation with respect to the Juno flyby at Ganymede. Juno's closest approach occurred at 16:56 UTC on 7 June 2021 in spacecraft event time which corresponds to 17:35 UTC Earth-received time considering the light travel time of 39 min. HST can only observe Ganymede when the moon is not occulted by Earth and when the South Atlantic Anomaly does not impede HST observations, which unfortunately occurred during an ~14 hr time window around the Juno flyby. The resulting available HST windows are shown in light blue in Figure 1. Ganymede's latitudinal position Ψ_m with respect to the center of Jupiter's magnetospheric plasma sheet is displayed as gray curve. The magnetic latitude Ψ_m is calculated based on a Jupiter centered tilted dipole model with $\Psi_m = 9.5^\circ \cos(\lambda_{III} - 200.8^\circ)$, where λ_{III} describes the system III longitude of Ganymede (Connerney et al., 1998; Dessler, 1983). Out of the available windows we scheduled the first three HST orbits directly after the Juno flyby. They are labeled orbit 1, 2, and 3 of visit 2 and started 2 hr 9 min after closest approach. Orbit 1 of visit 2 occurs when Ganymede is near maximum southern latitudes and then Ganymede moves toward the center of the plasma sheet and crosses it during orbit 3. Visit 1 was chosen to be symmetric to visit 2 in the sense that Ganymede covers approximately the same angular span $|\Psi_m|$ with respect to the plasma sheet. The reason is to better compare the emission pattern before and after the flyby. Observations during visit 1 ended 13 hr and 13 min before the Juno flyby.

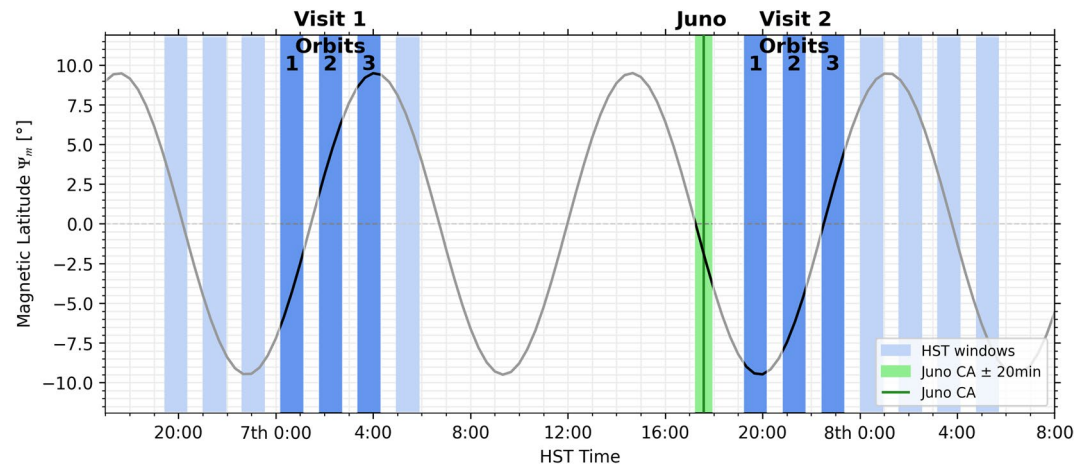


Figure 1. Schedule of Hubble Space Telescope (HST) observations with respect to Juno's Ganymede flyby. Juno's closest approach to Ganymede occurred on 7 June 2021 at 17:35 (UTC). Light blue areas display time windows when Ganymede is observable by HST. Executed HST observations (dark blue) consist of three orbits labeled 1, 2, and 3 in visit 1 before the flyby and three orbits labeled 1, 2, and 3 in visit 2 after the flyby. Magnetic latitude Ψ_m of Ganymede in Jupiter's magnetosphere is shown as gray curve.

3. Results

Ganymede's auroral emission at OI 1,356 Å for the three orbits of both visits is displayed in Figure 2. It demonstrates that the auroral emission on Ganymede's trailing hemisphere is primarily located at large northern and southern latitudes as known from previous observations (Feldman et al., 2000; McGrath et al., 2013; Musacchio et al., 2017).

3.1. Context for Juno

The HST observations taken before and after the Juno flyby provide context for the observations obtained by Juno. For each HST orbit, the disk averaged brightness of the OI 1,356 Å emission, including limb emission up to 200 km above the disk, is summarized in Table S1 in Supporting Information S1. The emission is brightest when Ganymede is near the center of Jupiter's magnetospheric plasma sheet, which occurs during orbit 1 of visit 1 (about 16 hr before the Juno flyby) and during orbit 3 of visit 2 (about 5 hr after the flyby). Ganymede was also near the center of plasma sheet during the Juno flyby. Orbit 1 of visit 1 displays an exceptional high average brightness of 132.8 ± 4.0 R, while during orbit 3 of visit 2 the brightness of 78.3 ± 2.6 R was typical, as compared to previous observations under similar conditions (Musacchio et al., 2017). Ganymede was not observed with HST during the Juno flyby, but the HST observations with the smaller temporal separation of 5 hr compared to 16 hr might more likely represent the state of its auroral emission while the flyby occurred.

3.2. Alternating North-South Brightness Ratio of Auroral Ovals

During orbit 1 of visit 1, Ganymede was below (i.e., south of) the plasma sheet (Figure 1). The HST observations displayed in Figure 2, left, reveal that the northern oval, which faces the center of the plasma sheet, was brighter than the southern oval. During orbit 2 of visit 1 Ganymede had moved above the plasma sheet and the southern oval, which then faced the center of the plasma sheet turned brighter. In the last orbit of visit 1, the emission is patchy and no hemisphere is clearly brighter than the other one. During orbit 1 and 2 of visit 2 Ganymede was below the plasma sheet and the northern oval was brighter (Figure 2, right). During orbit 3 of visit 2 Ganymede had moved above the plasma sheet and the southern oval turned brighter. This pattern demonstrates that the oval which faces the center of the plasma sheet is brighter than the oval which faces away from the plasma sheet.

The brightness of the northern and the southern ovals can be quantified by the average emission above 30° and below -30° latitude calculated within a disk which includes limb emission within 200 km above the surface. The resultant average hemispheric brightness is displayed in Figure 3 (for details on error bars see Supporting Information S1). The northern and southern brightness as a function of Ganymede's position with respect to the

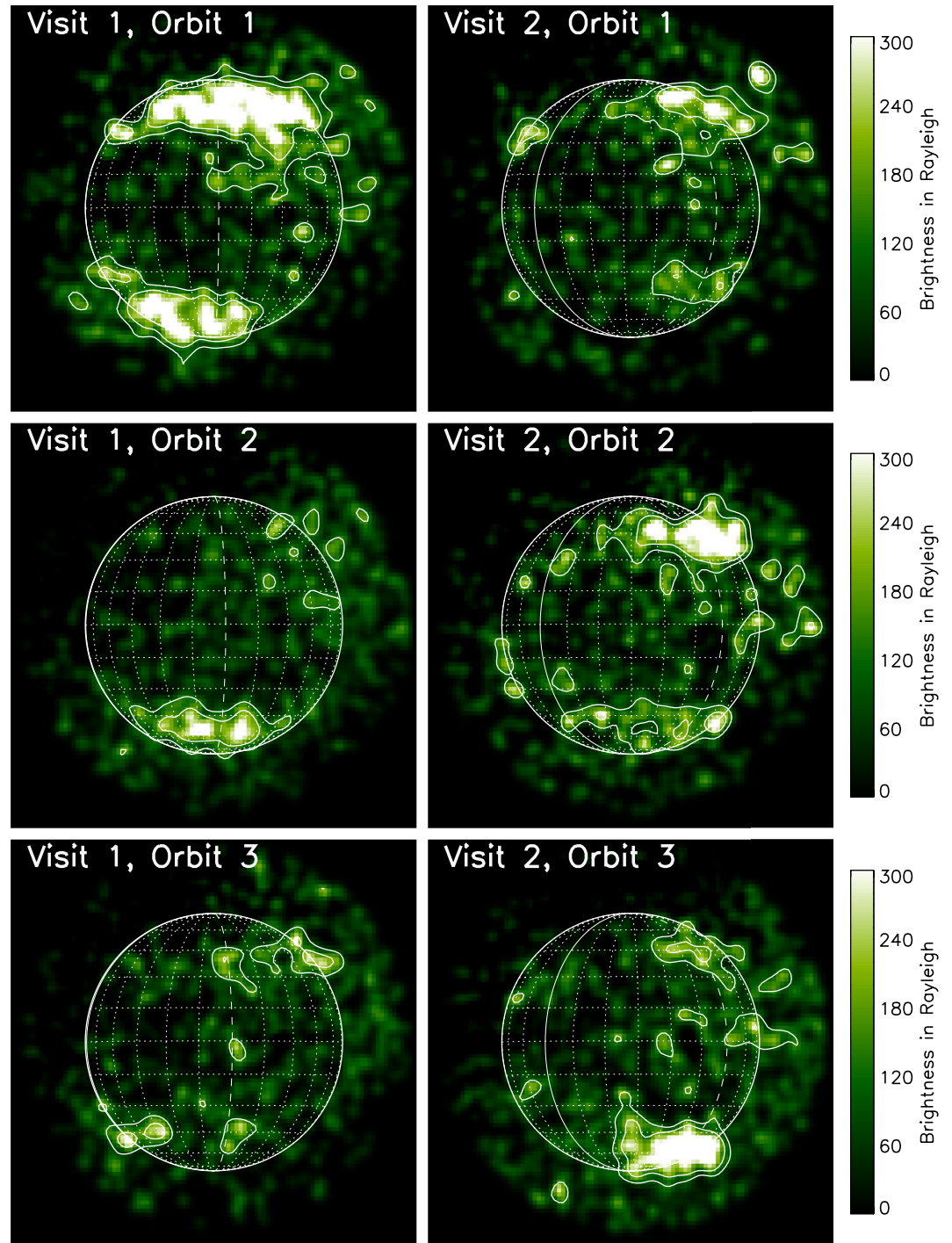


Figure 2. Hubble Space Telescope/STIS images of Ganymede's auroral brightness in Rayleigh at OI 1,356 Å. Visit 1 occurred before and visit 2 after the Juno flyby on 7 June 2021. Observations show mostly Ganymede's trailing, that is, plasma flow upstream, hemisphere. The dashed line indicates the 90° meridian.

plasma sheet (approximated by Jovian magnetic latitude Ψ_m) is shown in red and blue, respectively. The northern oval is brighter than the southern one when Ganymede is below the plasma sheet and vice versa when Ganymede is above. In the lower panel of Figure 3 we display the brightness ratio between north and south as light green solid line. The ratio with their error bars demonstrates that the asymmetry pattern is significant.

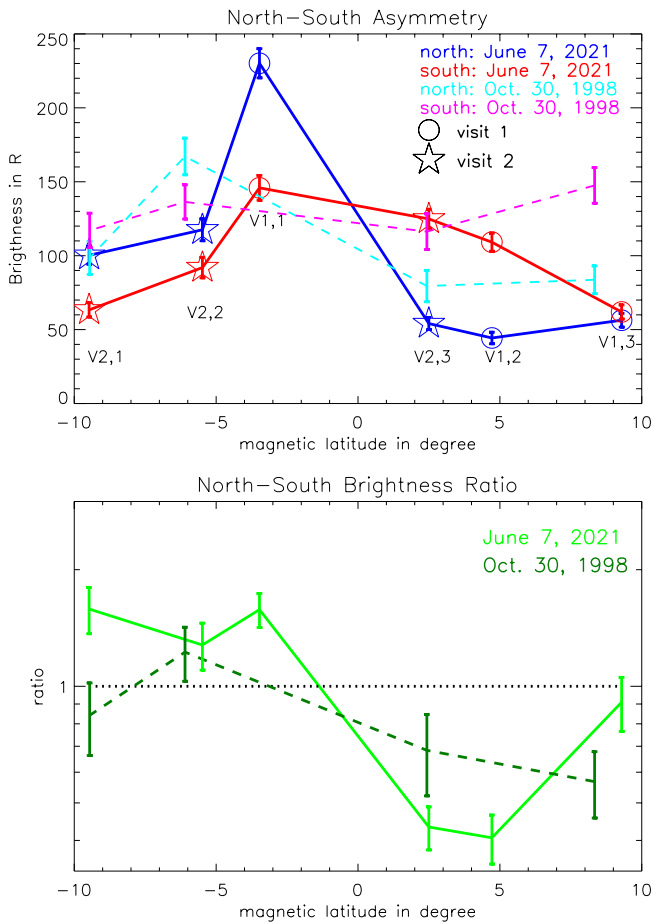


Figure 3. North-south asymmetry of Ganymede's auroral emission. Top panel: Average brightness of northern and southern hemispheres calculated above and below 30° latitude within a disk which includes the limb emission within 200 km. The abbreviations V1,1, V1,2, ... V2,3 refer to visit 1 orbit 1, visit 1 orbit 2, ... visit 2 orbit 3. Bottom panel: North-South brightness ratio.

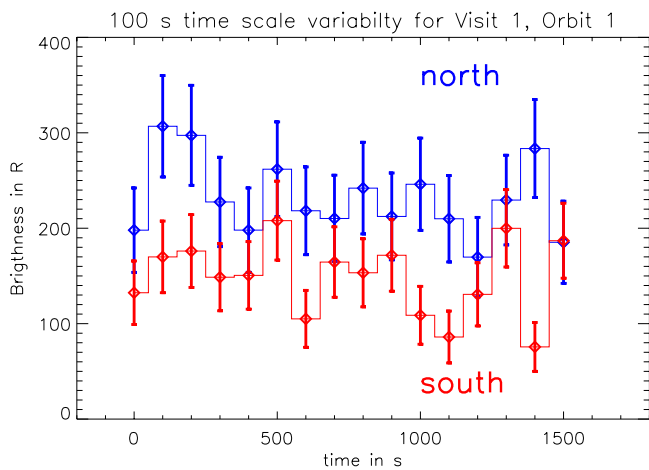


Figure 4. Short time scale analysis of intensities measured during orbit 1 of visit 1 on 7 June 2021. The northern and southern ovals are analyzed separately.

Ganymede's trailing side had been observed previously by HST/STIS on 30 October 1998 (Feldman et al., 2000). The north-south asymmetry of these observations is shown in Figure 3 as turquoise and pink dashed lines in the top panel and the associated ratios in dark green in the lower panel. Out of the four HST orbits in the 1998 data set, three orbits follow the same asymmetry trend as the 2021 data while one orbit at large negative latitudes shows no asymmetry within the error bars (see left dark green data points in Figure 3). These values are consistent with the analysis of quadrants as function of Ψ_m in Musacchio et al. (2017). Generally speaking, the 1998 data supports the conclusion that the north-south brightness ratio alternates with Ganymede's position in Jupiter's plasma sheet such that the hemisphere facing the center of the plasma sheet is brighter than the opposite hemisphere. The associated period is the synodic rotation period of Jupiter in the rest frame of Ganymede, which is 10.54 hr.

3.3. Short Time Scale Variability

The STIS images of Ganymede's auroral emission in Figure 2 are patchy and thus appear to represent small-scale temporal variability. Therefore we investigate if temporal variability on time-scales shorter than an HST orbit of ~ 40 min can be resolved. In Figure 4, we show the brightness within sub-exposures of 100 s length. The brightness is calculated above 30° and below -30° latitudes within a disk including 200 km above the limb. The sub-exposures displayed in Figure 4 are from the HST orbit with the brightest emission of the 7 June 2021 data, that is, orbit 1 of visit 1 (top left in Figure 2). Some of the brightness values b_i of the 100 s sub-exposures i differ beyond the one-sigma error bars. This is, however, not sufficient to demonstrate true time-variability. For a simple test we calculate the standard deviation $\sigma_{\text{sub-exp}} = \left[1/(N-1) \sum (\bar{b} - b_i)^2\right]^{1/2}$ of the sub-exposures (with $\bar{b} = 1/N \sum_N b_i$) and compare it with the averaged one-sigma uncertainty $\bar{\sigma}_{\text{indiv}} = 1/N \sum_N \sigma_i$ of each of the N sub-exposures with σ_i being the uncertainty of subexposure i . Real time-variability would be indicated if $r = \sigma_{\text{sub-exp}}/\bar{\sigma}_{\text{indiv}} > 1$, that is, the variability between the sub-exposures is larger than their individual error bars. The brightness evolution of the northern ovals in Figure 4 is characterized by $r = 0.84$ indicating that the observations are consistent with a time-constant emission. The southern oval has a ratio of $r = 1.1$ indicating possible time-variability. However, averaging over all six HST orbits we find $r = 0.91$ for the northern oval and 0.99 for the southern oval. Detailed statistical values for all orbits can be found in Table S2 in Supporting Information S1. The r -values thus imply no clear sign of short-term variability of 100 s. Further, more sophisticated tests are required to derive stronger conclusions.

3.4. Auroral Brightness and Required Electron Energy Fluxes

An auroral brightness on Ganymede of 100 R at OI 1,356 Å can be explained following Eviatar et al. (2001) by an electron population with surface density of $100 \times 10^6 \text{ m}^{-3}$ and temperature of 100 eV within an O_2 column density of $3 \times 10^{18} \text{ m}^{-2}$ (see Figure S1 in Supporting Information S1). For intense brightness values of 1,000 R such as seen by Juno (Greathouse et al., 2022), an electron density with $950 \times 10^6 \text{ m}^{-3}$ and a temperature of 200 eV are required (Figure S1 in Supporting Information S1). Assuming a Maxwellian distribution, we can calculate the associated energy flux in one-direction as

$(4\pi)^{-1/2} m_e n_e (2k_B T_e / m_e)^{3/2}$, which assumes 5.4 mW m^{-2} for the 100 R and 140 mW m^{-2} for the 1000 R cases, respectively (with the electron mass m_e and the Boltzmann constant k_B). Up to a neutral column density of $3 \times 10^{19} \text{ m}^{-2}$ the atmosphere is “optically thin” for electrons and thus a 10 times smaller electron density within a 10 times larger neutral column density leads to the same brightness values. Thermal ionospheric electrons are expected to be much colder and electrons and the neutrals are approximately collisionless in Ganymede's atmosphere and ionosphere (Eviatar et al., 2001). Electrons within the downward going loss cone will thus be lost to the surface as seen in JADE and JEDI data (Allegrini et al., 2022; Clark et al., 2022). Therefore an energy flux from the magnetosphere into the atmosphere/ionosphere on the order of $10\text{--}100 \text{ mW m}^{-2}$ is required to produce the brightnesses of Ganymede's aurora. The electrons need to be accelerated in the vicinity of Ganymede since the electron energy density in Jupiter's magnetosphere near Ganymede is insufficient to produce the aurora (Eviatar et al., 2001).

The brightness of Jupiter's main aurora is on the order of several 100 kR. The energy fluxes required to produce 100 kR at Jupiter are $\sim 10 \text{ mW m}^{-2}$ (Gustin et al., 2016; Mauk et al., 2017). Thus for similar energy fluxes, the efficiency to produce auroral emission in Jupiter's atmosphere is on the order of 10^3 times larger than in Ganymede's atmosphere. This difference can alternatively be demonstrated by considering Ganymede's FUV luminosity of $\sim 3 \times 10^7 \text{ W}$ (Saur et al., 2021). Assuming the emission originates from 10% of Ganymede's area, the emitted energy flux is $3.5 \times 10^{-6} \text{ W m}^{-2}$. For electron fluxes on the order of $10\text{--}100 \text{ mW m}^{-2}$, this would correspond to an efficiency to convert electron energy into FUV emission of $\sim 10^{-4}$, which is a factor of 10^2 to 10^3 smaller compared to the FUV efficiency of Jupiter's main aurora in the range $10^{-1}\text{--}10^{-2}$ (Bhardwaj & Gladstone, 2000; Mauk et al., 2017). The primary reasons for the difference are: (a) Jupiter's atmosphere is collisionally thick and energetic electrons deposit all of their energy in the upper atmosphere while Ganymede's atmosphere is collisionally thin and most electrons are lost to the surface of Ganymede. (b) In Jupiter's hydrogen atmosphere about 10%–20% of electron energy is radiated in FUV H_2 band emissions, but only about 1% of the energy of electrons interacting with Ganymede's oxygen atmosphere is radiated away as OI 1,356 Å photons and most of the energy is spent in ionization and dissociation of O_2 .

4. Conclusions and Discussion

HST observations of Ganymede taken on 7 June 2021 provide context for the flyby of the Juno spacecraft at Ganymede. Based on the HST observations closest to the flyby, Ganymede's auroral emission and thus its magnetospheric particle environment appear to have been in a typical state (i.e., similar to previous observations) during the Juno flyby.

The analysis of the HST observations for Ganymede's trailing hemisphere shows that the brightness ratio of the northern and southern ovals oscillate such that the hemisphere facing Jupiter's plasma sheet is brighter. This suggests that the properties of the surrounding plasma sheet in the northern and southern direction control the brightness of Ganymede's aurora. In case of Io and Europa, an asymmetry in the north-south limb UV emission was observed as well (Retherford et al., 2003; Roth et al., 2014, 2016). The underlying reason for the asymmetry in case of Io and Europa was attributed to the larger electron thermal energy reservoir on the side facing the surrounding plasma sheet. However, in case of Ganymede the cause of the asymmetric auroral emission cannot be attributed to the properties of Jupiter's magnetospheric electrons. Due to the low plasma density at Ganymede's orbit, these magnetospheric electrons do not possess a sufficiently large energy density to cause Ganymede's aurora (Eviatar et al., 2001). Therefore other energy fluxes into Ganymede's magnetosphere and a local electron energization process are needed in contrast to Europa and Io where the electron energy density in the surrounding plasma is sufficient to power their auroral emission.

The plasma density in Jupiter's plasma sheet is a property which changes in the north-south direction above and below Ganymede, while the plasma velocity in this direction is relatively similar (Bagenal & Delamere, 2011). The gradient of the plasma density results in a larger plasma momentum on the side facing the center of the plasma sheet. Close to Ganymede, the plasma is slowed due to the interaction of Jupiter's magnetospheric plasma with Ganymede's internal magnetic field and the collisions with its atmosphere. Since Ganymede and the surrounding plasma are connected by magnetic field lines, the slowed plasma in Ganymede's vicinity and the fast flowing plasma above and below Ganymede is generating magnetic stresses around Ganymede. On the side with the larger momentum, the magnetic stresses are larger. The larger momentum also causes the Alfvén wings on that

side to be more strongly bent back compared to the other hemisphere. The bent-back angle is proportional to the square root of the plasma density (Neubauer, 1980; Saur et al., 2013). The larger bend and the larger stresses are associated with larger electromagnetic energy fluxes between the denser side of the plasma sheet and Ganymede. These energy fluxes thus appear to be the root power source for the auroral emission. The asymmetric stresses are also the cause for larger electric currents feeding into Ganymede's magnetosphere on the associated hemisphere. However, the electric currents enter the Ganymede system primarily on the flanks of Ganymede and not on the upstream and downstream side where auroral emission is observed (Duling et al., 2014, 2022; Jia et al., 2008; Neubauer, 1998). Reconnection might also be asymmetric within an inhomogeneous background plasma but the scales of the gradient of the background properties are large compared to the size of Ganymede. We therefore suggest that the asymmetric plasma momentum causes asymmetric magnetic stresses with associated asymmetric electromagnetic energy fluxes toward Ganymede. These fluxes ultimately provide the power for Ganymede's auroral acceleration processes and its auroral emission.

Our simple analysis of 100 s sub-exposures reveal no statistically significant time-variability of the total auroral brightness on short time scales. However, further studies with more sophisticated tests and better resolved observations such as with JUICE (e.g., Grasset et al., 2013) are warranted to detect possible short term variability not resolved in this study.

Data Availability Statement

This work is based on observations with the NASA/ESA Hubble Space Telescope obtained at the Space Telescope Science Institute, which is operated by the Association of Universities for Research in Astronomy (AURA), Inc., under NASA contract NAS 5–26555. All data used in this study is available on the Mikulski Archive for Space Telescopes (MAST) of the Space Telescope Science Institute at <http://archive.stsci.edu/hst/>. The specific data sets are listed in Table S1 in Supporting Information S1 and can be accessed at https://mast.stsci.edu/search/ui/#/hst/results?resolve=true&radius=3&radius_units=arcminutes&data_type=all&observations=S&active_instruments=stis,acs,wfc3,cos,fgs&legacy_instruments=foc,fos,ghrs,hsp,nicmos,wfpc,wfpc2&proposal_id=I6499&select_cols=ang_sep,sci_aper_1234,sci_central_wavelength,sci_data_set_name,sci_dec,sci_actual_duration,sci_spec_1234,sci_hlsp,sci_instrume,sci_pi_last_name,sci_preview_name,sci_pep_id,sci_ra,sci_refnum,sci_release_date,scp_scan_type,sci_start_time,sci_stop_time,sci_targetname&useStore=false&search_key=819f8c5cea95f.

References

- Allegrini, F., Bagenal, F., Ebert, R. W., Louarn, P., McComas, D. J., Szalay, J. R., et al. (2022). Plasma observations during the 7 June 2021 Ganymede flyby from the Jovian Auroral Distributions Experiment (JADE) on Juno. *Geophysical Research Letters*, *49*, e2022GL098682. <https://doi.org/10.1029/2022GL098682>
- Bagenal, F., & Delamere, P. A. (2011). Flow of mass and energy in the magnetospheres of Jupiter and Saturn. *Journal of Geophysical Research*, *116*(A5), A05209. <https://doi.org/10.1029/2010JA016294>
- Bhardwaj, A., & Gladstone, G. R. (2000). Auroral emissions of the giant planets. *Review of Geophysics*, *38*(3), 295–353.
- Clark, G., Kollmann, P., Mauk, B. H., Paranicas, C., Haggerty, D., Rymer, A., et al. (2022). Energetic charged particle observations during Juno's close flyby of Ganymede. *Geophysical Research Letters*, *49*, e2022GL098572. <https://doi.org/10.1029/2022GL098572>
- Connerney, J. E. P., Acuna, M. H., Ness, N. F., & Satoh, T. (1998). New models of Jupiter's magnetic field constrained by the Io flux tube footprint. *Journal of Geophysical Research*, *103*(A6), 11929–11939. <https://doi.org/10.1029/97ja03726>
- Dessler, A. J. (1983). *Physics of the Jovian magnetosphere*. Cambridge University Press.
- Duling, S., Kurth, W. S., Sulaiman, A. H., Mauk, B. H., Bolton, S. J., & Louis, S. (2022). Ganymede MHD model: Magnetospheric context for Juno's PJ34 flyby. *Geophysical Research Letters*, *49*, e2022GL101688. <https://doi.org/10.1029/2022GL101688>
- Duling, S., Saur, J., & Wicht, J. (2014). Consistent boundary conditions at nonconducting surfaces of planetary bodies: Applications in a new Ganymede MHD model. *Journal of Geophysical Research*, *119*(6), 4412–4440. <https://doi.org/10.1002/2013JA019554>
- Eviatar, A., Strobel, D. F., Wolfven, B. C., Feldman, P., McGrath, M. A., & Williams, D. J. (2001). Excitation of the Ganymede ultraviolet aurora. *The Astrophysical Journal*, *555*(2), 1013–1019. <https://doi.org/10.1086/321510>
- Feldman, P. D., McGrath, M. A., Strobel, D. F., Moos, H. W., Retherford, K. D., & Wolfven, B. C. (2000). HST/STIS ultraviolet imaging of polar aurora on Ganymede. *The Astrophysical Journal*, *555*(2), 1085–1090. <https://doi.org/10.1086/308889>
- Grasset, O., Dougherty, M. K., Coustenis, A., Bunce, E. J., Erd, C., Titov, D., et al. (2013). Jupiter ICy moons Explorer (JUICE): An ESA mission to orbit Ganymede and to characterise the Jupiter system. *Planetary and Space Science*, *78*, 1–21. <https://doi.org/10.1016/j.pss.2012.12.002>
- Greathouse, T., Gladstone, R., Molyneux, P., Versteeg, M., Hue, V., Kammer, J., et al. (2022). UVS observations of Ganymede's aurora during Juno orbits 34 and 35. *Geophysical Research Letters*, *49*, e2022GL099794. <https://doi.org/10.1029/2022GL099794>
- Gustin, J., Grodent, D., Ray, L. C., Bonfond, B., Bunce, E. J., Nichols, J. D., & Ozak, N. (2016). Characteristics of north jovian aurora from STIS FUV spectral images. *Icarus*, *268*, 215–241. <https://doi.org/10.1016/j.icarus.2015.12.048>
- Hall, D. T., Feldman, P. D., McGrath, M. A., & Strobel, D. F. (1998). The far-ultraviolet oxygen airglow of Europa and Ganymede. *The Astrophysical Journal*, *499*(5), 475–481. <https://doi.org/10.1086/305604>

Acknowledgments

J.S. appreciates the help of William Januszewski and Joleen Carlberg from STScI in scheduling the observations. This project has received funding from the European Research Council (ERC) under the European Union's Horizon 2020 research and innovation programme (grant agreement No. 884711). DFS is supported by STScI HST-GO-16499.006-A grant under NASA contract NAS5-26555. Some of this research was carried out at the Jet Propulsion Laboratory, California Institute of Technology, under contract with NASA (80NM0018D0004).

- Jia, X., Walker, R., Kivelson, M., Khurana, K., & Linker, J. (2008). Three-dimensional MHD simulations of Ganymede's magnetosphere. *Journal of Geophysical Research*, *113*, A06212.
- Kivelson, M. G., Khurana, K. K., Walker, R. J., Russell, C. T., Linker, J. A., Southwood, D. J., & Polansky, C. (1996). A magnetic signature at Io: Initial report from the Galileo magnetometer. *Science*, *273*, 337–340.
- Kivelson, M. G., Warnecke, J., Bennett, L., Joy, S., Khurana, K. K., Linker, J. A., et al. (1998). Ganymede's magnetosphere: Magnetometer overview. *Journal of Geophysical Research*, *103*(E9), 19963–19972. <https://doi.org/10.1029/98JE00227>
- Mauk, B. H., Haggerty, D. K., Paranicas, C., Clark, G., Kollmann, P., Rymer, A. M., et al. (2017). Juno observations of energetic charged particles over Jupiter's polar regions: Analysis of monodirectional and bidirectional electron beams. *Geophysical Research Letters*, *44*(10), 4410–4418. <https://doi.org/10.1002/2016GL072286>
- McGrath, M. A., Jia, X., Retherford, K. D., Feldman, P. D., Strobel, D. F., & Saur, J. (2013). Aurora on Ganymede. *Journal of Geophysical Research*, *118*(5), 2043–2054. <https://doi.org/10.1002/jgra.50122>
- Musacchio, F., Saur, J., Roth, L., Retherford, K. D., McGrath, M. A., Feldman, P. D., & Strobel, D. F. (2017). Morphology of Ganymede's FUV auroral ovals. *Journal of Geophysical Research*, *122*(3), 2855–2876. <https://doi.org/10.1002/2016JA023220>
- Neubauer, F. M. (1980). Nonlinear standing Alfvén wave current system at Io: Theory. *Journal of Geophysical Research*, *85*(A3), 1171–1178. <https://doi.org/10.1029/ja085ia03p01171>
- Neubauer, F. M. (1998). The sub-Alfvénic interaction of the Galilean satellites with the Jovian magnetosphere. *Journal of Geophysical Research*, *103*(E9), 19843–19866. <https://doi.org/10.1029/97je03370>
- Retherford, K. D., Moos, H. W., & Strobel, D. F. (2003). Io's auroral limb glow: Hubble Space Telescope FUV observations. *Journal of Geophysical Research*, *108*(A8), 1333. <https://doi.org/10.1029/2002JA009710>
- Roth, L., Ivchenko, N., Gladstone, G. R., Saur, J., Grodent, D., Bonfond, B., & Retherford, K. D. (2021). A sublimated water atmosphere on Ganymede detected from Hubble Space Telescope observations. *Nature Astronomy*, *5*(10), 1043–1051. <https://doi.org/10.1038/s41550-021-01426-9>
- Roth, L., Saur, J., Retherford, K. D., Feldman, P. D., & Strobel, D. F. (2014). A phenomenological model of Io's UV aurora based on HST/STIS observations. *Icarus*, *228*, 386–406. <https://doi.org/10.1016/j.icarus.2013.10.009>
- Roth, L., Saur, J., Retherford, K. D., Strobel, D. F., Feldman, P. D., McGrath, M. A., et al. (2016). Europa's far ultraviolet oxygen aurora from a comprehensive set of HST observations. *Journal of Geophysical Research*, *121*(3), 2143–2170. <https://doi.org/10.1002/2015JA022073>
- Saur, J., Duling, S., Roth, L., Jia, X., Strobel, D. F., Feldman, P. D., et al. (2015). The search for a subsurface ocean in Ganymede with Hubble Space Telescope observations of its auroral ovals. *Journal of Geophysical Research*, *120*(3), 1715–1737. <https://doi.org/10.1002/2014JA020778>
- Saur, J., Grambusch, T., Duling, S., Neubauer, F. M., & Simon, S. (2013). Magnetic energy fluxes in sub-Alfvénic planet star and moon planet interactions. *Astronomy & Astrophysics*, *552*, A119. <https://doi.org/10.1051/0004-6361/201118179>
- Saur, J., Janser, S., Schreiner, A., Clark, G., Mauk, B. H., Kollmann, P., et al. (2018). Wave-particle interaction of Alfvén waves in Jupiter's magnetosphere: Auroral and magnetospheric particle acceleration. *Journal of Geophysical Research*, *123*(11), 9560–9573. <https://doi.org/10.1029/2018JA025948>
- Saur, J., Willmes, C., Fischer, C., Wennmacher, A., Roth, L., Youngblood, A., & Reiners, A. (2021). Brown dwarfs as ideal candidates for detecting UV aurora outside the Solar System: Hubble Space Telescope observations of 2MASS J1237+6526. *Astronomy & Astrophysics*, *655*, A75. <https://doi.org/10.1051/0004-6361/202040230>

References From the Supporting Information

- Bevington, P. R., & Robinson, D. K. (2003). *Data reduction and error analysis for the physical sciences*. McGraw Hill.
- Hall, D. T., Strobel, D. F., Feldman, P. D., McGrath, M. A., & Weaver, H. A. (1995). Detection of an oxygen atmosphere on Jupiter's moon Europa. *Nature*, *373*(6516), 677–679. <https://doi.org/10.1038/373677a0>
- Kanik, I., Norem, C., Makarov, O., Palle, P. V., Ajello, J., & Shemansky, D. (2003). Absolute emission cross sections of OI (130.4 nm) and OI (135.6 nm). *Journal of Geophysical Research*, *108*(E11), 5126. <https://doi.org/10.1029/2000je001423>